15th Canadian Masonry Symposium
Ottawa, Canada
June 2-5, 2025

Raising Code Limits on Specified Reinforcement Strength by Adoption of High-Strength Steel Bars (HSRBs) in Structural Masonry

Dimitrios Kalliontzis[i], Waleed Khan[ii], Samvid Parajuli[iii], and Omar Khalid[iv]

ABSTRACT

In the United States, the adoption of high-strength non-prestressed reinforcing bars (HSRBs) in design was initiated by the reinforced concrete industry through ACI 318. The adoption was motivated by several factors including the ability to increase bar spacings, reduce steel congestion, reduce construction materials and costs, and minimize the building carbon footprint. It appears that this trend is continuing with the increasing availability of reinforcement of higher grades, making it imperative that the masonry industry be able to adapt. To ensure that the masonry industry adapts to these new developments, the University of Houston has embarked on a research program to investigate the feasibility of HSRBs in structural masonry design. This paper presents an overview of this program and current findings. So far, the program has completed a series of laboratory tests to evaluate existing TMS 402/602-22 provisions on lap-splice length and flexural design. Lap-splice tests indicated the need to incorporate a reinforcement grade factor of 1.15 for Grade 80 bars in the existing provisions. Lap-splice tests also showed the need to revisit the accuracy of the reinforcement size factor, as it is conservative for smaller and liberal for larger bar diameters. Out-of-plane wall tests were used to evaluate the flexural behavior of masonry walls with longitudinal HSRBs. The test results indicated that TMS 402/602-22, modified to account for Grade 80 bars, can provide satisfactory estimates of nominal strength with sufficient conservatism with respect to the experimental responses. Finally, the research program has performed several prototype beams, columns, walls, and full-scale building designs to investigate the potential benefits of utilizing HSRBs in masonry construction. Findings showed that reductions in reinforcing material costs can reach 25% by using Grade 80 versus Grade 60 bars. These benefits can be further increased considering reductions in material weights and cell grouting.

KEYWORDS

High-strength steel, Grade 80, ASTM 706, ASTM 615, lap splice, flexure, concrete masonry, clay brick.

[i] Assistant Professor, University of Houston, Houston, Texas, United States, dkallion@central.uh.edu
[ii] Graduate Student, University of Houston, Houston, Texas, United States, mkhan88@CougarNet.uh.edu
[iii] Graduate Student, University of Houston, Houston, Texas, United States, sparaju2@CougarNet.uh.edu
[iv] Formerly at the University of Houston as a Graduate Student, Houston, Texas, United States, onkhalid@CougarNet.uh.edu

MOTIVATION

High strength reinforcing bars (HSRBs) are those with a specified yield strength greater than or equal to 80,000 psi (550 MPa). HSRBs are typically produced with minimum yield strengths of 80,000 psi (550 MPa) and 100,000 psi (690 MPa), namely: Grade 80 and Grade 100 reinforcing bars, respectively. ASTM A706 [2] and A615 [3] are the most used specifications for reinforcing bars in structural masonry, differing notably in the required chemical composition and mechanical properties. A706 steel contains lower carbon content than A615 steel, resulting in a softer material with enhanced ductility. The intent to use HSRBs in masonry design is motivated by the reduction in material and construction cost, reduction in bar size or increase in longitudinal bar spacing, and, overall, reduction in the carbon footprint of masonry structures, which is a high need of the contemporary building industry. It is also noted that HSRBs of Grade 80 and Grade 100 are as available as Grade 60 reinforcing bars in most markets in the United States and elsewhere.

Grade 60 and Grade 80 bars (Fig. 1) have an average price difference of 4% (Khalid and Kalliontzis [4]), while there is no measurable difference in the energy consumption required to fabricate either of the two bar grades. In their 2023 TMS journal publication, Khalid and Kalliontzis [4] showed that material cost reductions on the order of 25% can be achieved with the use of Grade 80 versus Grade 60 bars in masonry buildings, with equivalent reductions in the carbon footprint up to 33%.

(a) Bar coupon setup

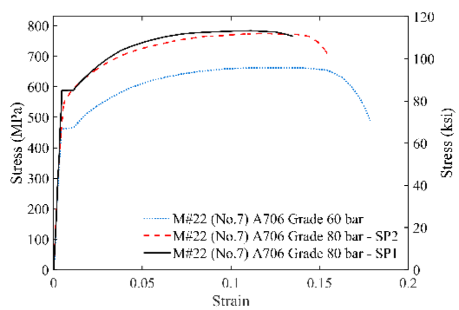

(b) Engineering stress-strain curves

Figure 1: (a) Coupon setup per ASTM A370 [5] and (b) engineering stress-strain curves for Grade 60 and Grade 80 No. 5 A706 deformed bars [7].

Table 1 presents a cost evaluation study from [4] using a JHM box retail store prototype design with Grade 60 bars, which was redesigned with Grade 80 bars. The study demonstrated an overall reduction in the cost of reinforcing steel materials by 25% due to the use of Grade 80 versus Grade 60 bars. However, it was noted that additional cost reductions would result from the reduced weight of materials being handled, and from either reducing the cell grouting by spreading the bars further apart, or by using smaller diameter bars which are easier to handle in construction and require shorter lap lengths.

Fig. 2 compares the normalized nominal moment corresponding to the use of Grade 60 versus Grade 80 bars for $f'_m = 17.2$ MPa (2,500 psi). The nominal moment for Grade 80 bars is consistently larger than that of Grade 60 bars for the same reinforcement ratio, while their difference increases with the reinforcement ratio. This increase in nominal bending moment can be utilized to reduce the number of reinforcing bars, or bar sizes, especially in tension-controlled members.

All in all, the adoption of HSRBs in masonry design is vital to address the transition to higher steel grades by the building industry, which is often combined with the abandonment of lower bar grades (ACI 318-19 [1]). Adopting Grade 80 bars constitutes a first step toward HSRBs and a straightforward way to reduce the carbon footprint of masonry buildings by reducing the number of reinforcing bars. This paper summarizes research findings and recommendations on lap-splice length requirements and flexural behavior that can incentivize the adoption of Grade 80 reinforcing bars in structural masonry design.

Table 1: Cost Evaluation for JHM Box Retail Store Structure: Grade 60 versus 80 bars [4].

Design	Bar size	Grade 60 No. 5 bars		Bar size	Grade 80 No. 4/5 bars	
		Required length, m	Price, $		Required length, m	Price, $
Out-of-plane, load bearing	No.5	6,125	28,133	No.4	6,110.3	19,044.65
Out-of-plane, non-load bearing	No.5	224.3	1,030.4	No.4	223.4	696.35
Lintel above entrance	No.5	515.1	2,366	No.4	514.5	1,603.6
Other lintel beams	No.5	8.5	39.2	No.4	8.5	26.6
Shear wall	No.5	1,396.6	6,414.8	No.5	1,481	7,191.32
Retaining wall	No.5	102.4	470.4	No.4	76.8	239.4
Total =	-	8,371.9	**38,453.8**	-	8,414.5	**28,801.92**

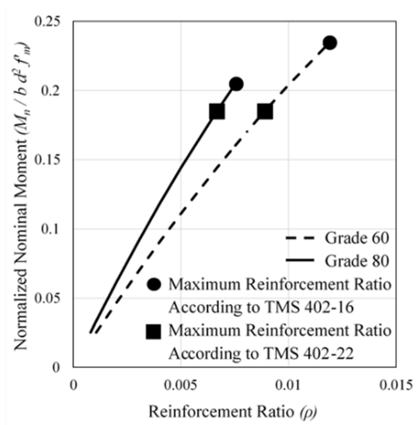

Figure 2: Normalized nominal moment versus reinforcement ratio by expanding the existing TMS 402/602 specifications to Grade 80 bars [4, 6].

LAP-SPLICE LENGTH REQUIREMENT FOR GRADE 80 BARS

A series of computational and experimental studies has been performed to evaluate the lap-splice length requirements of Grade 80 bars in concrete and clay brick masonry [7]. The studies included twenty-two test specimens, with test variables being the bar size, the lap-splice length, and the ASTM designation of the bars (A706 and A615). The tests were followed by a parametric numerical analysis study to investigate additional variables related to bar sizes and lap-splice lengths.

The test setup for the lap-splice tests is presented in Fig. 3. This setup was adopted from Thompson [8] and it has also been used by many other researchers to characterize lap-splice length requirements in masonry. The setup included two I-section steel columns securely anchored to the laboratory strong floor. Four cross I-beams were installed on the top and bottom of the columns to support anchorage of the reinforcing bars and application of the bar pullout forces using two POWER TEAM hydraulic jacks (J1 and J2). The masonry panels were placed in the center of the frame and included two symmetric contact lap-splice coupons to negate bending moments that could be produced by the bar force couples in each splice. As such, the test setup ensured a direct tension demand to the panel system to avoid confinement effects due to stress gradients that are present in lap-splice test schemes that induce a flexural demand to the splice [9].

To synchronize the load application, the two hydraulic jacks (J1 and J2) were connected to an electrical Power Team single-acting gasoline hydraulic pump PG553 through a T-connector. Eight Grade 80 ZAP SCREWLOK FX shear screw couplers (C1-C8) were used to mount the masonry panel to the top and bottom of the frame by anchorage of the reinforcing bars. Each bar end was inserted with the same length into the coupler sleeve and bolted to transfer tension stresses via interlocking between the bolts and the bar.

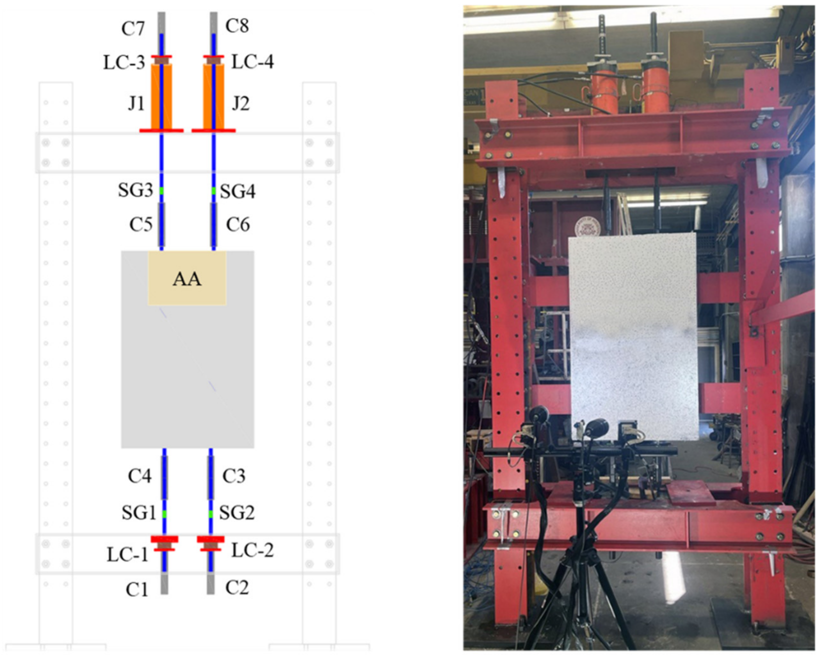

AA: ARAMIS monitor area; C: Coupler; J: Hydraulic Jack; LC: Load Cell; and SG: Strain gauge

Figure 3: Test setup and instrumentation of lap-splice tests [7].

The objective of the experiments from Fig. 3 was to measure a reinforcement grade factor, Ψ_g, for use with the existing lap-splice equation of TMS 402:

$$(1)\quad l_d = \frac{0.13 d_b^2 f_y \gamma}{K\sqrt{f'_m}} \Psi_g \geq 12.0 \text{ in } (= 0.3 \text{ m})$$

where l_d is the design lap-splice length; d_b is the nominal bar diameter in inches (1.0 inch = 25.4 mm); f_y is the nominal yield strength of the lap-spliced bar in psi (1.0 psi = 0.0069 MPa); γ is the bar size factor; K is the bar clear spacing and cover factor; and f'_m is the masonry compressive strength in psi. The parameter Ψ_g in Eq. [1] is taken as 1.0 in TMS 402-22 for Grade 40 and 60 bars. Per ACI 318-19, Ψ_g is defined as 1.15 and 1.30 for Grade 80 and Grade 100 bars, respectively, with reference to the development length equations in Table 25.4.2.3 of ACI 318-19 [1].

Eq. [1] was developed so that the spliced bars attain a stress greater than or equal to $1.25 f_y$. The 1.25 factor imposed on the nominal yield strength originates from an assumed design criterion that dates to the 2002 MSJC code [10]. This criterion was anecdotally introduced to ensure that the spliced bars develop adequate ductility and that each bar exceeds the actual yield strength, which can reach 500 MPa (72 ksi) for reinforcing bars that are fabricated as Grade 60 (i.e., 72/60 = 1.2 < 1.25).

A summary of the Grade 80 lap-splice test results from [7] is presented in Fig. 4. Combining these results with additional numerical analysis data performed by Khalid et al. [7], it was concluded that Grade 80 A706 bars of all bar sizes and Grade 80 A615 of No. 6 or smaller diameters can satisfy the $1.25f_y$ design criterion using $\Psi_g = 1.0$ in Eq. [1]. However, A615 bars of No. 7, which are primarily used in low-seismic regions, failed the design criterion of $1.25f_y$ with $\Psi_g = 1.0$ or $\Psi_g = 1.15$. This discrepancy was attributed, in part, to the less controlled properties of A615 bars that result in less ductile behavior and less dependable performance. An additional reason for this discrepancy was the definition of γ in Eq. [1] which tends to produce overly conservative lengths for smaller bar diameters and liberal lengths for larger bars [10]. Since A615 bars are customarily used in low-seismic regions with lower ductility demands, the requirement of an added safety factor of 1.25 to develop f_y is excessive and places an unnecessary constraint on masonry construction. It is therefore recommended to reduce this safety factor but keep it to an acceptable value. This need is further emphasized by experimental measurements showing that the actual yield strength of Grade 80 bars is unlikely to exceed 90.5 ksi (i.e., $90.5/80 = 1.13 < 1.15$) according to the rigorous rebar test series reported by Overby et al. [11]. Thus, a factor lower than 1.25 can provide a dependable lap splice that exceeds the actual yielding strength of Grade 80 bars. As a result, a reduced design criterion of $1.15f_y$ is recommended for spliced Grade 80 A615 bars which is sufficient to attain and reliably surpass the upper yield point of Grade 80 bars. By reducing the limit, Eq. [1] can be modified using $\Psi_g = 1.15$ for all ASTM Grade 80 bars.

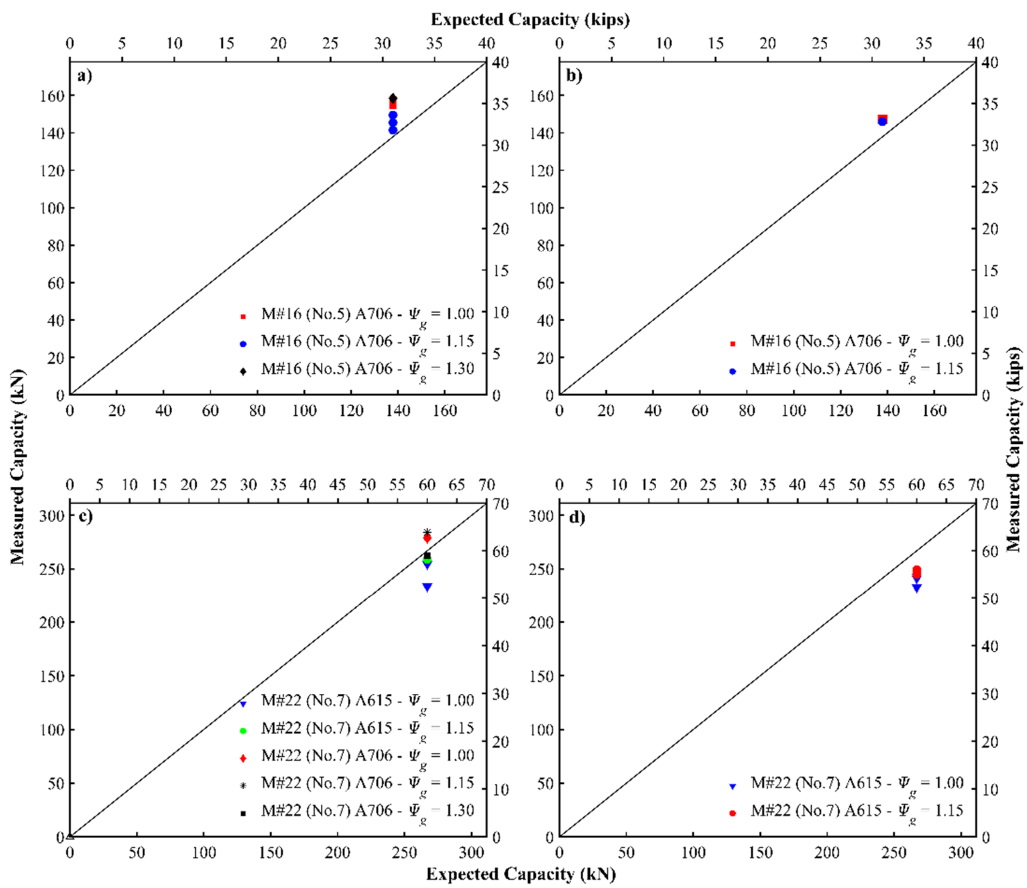

Figure 4: Expected versus measured lap-splice length capacities: (a) CMU with No. 5 bars; (b) CB with No. 5 bars; (c) CMU with No. 7 bars; and (d) CB with No. 7 bars. [7]; CMU = Concrete Masonry Unit; CB = Clay Brick.

Fig. 5 presents collectively the experimental and numerical lap-splice length data by Khalid et al. [7] in terms of four Quadrants [10] that measure the conservatism of Eq. [1] for Grade 80 bars with reference to $\Psi_g = 1.15$ and the design criterion of $1.15f_y$. The data included Grade 80 bars from No. 4 to No. 7 bars and f'_m values from 13.8 MPa (2,000 psi) to 27.6 MPa (4,000 psi). Quadrants I and III indicate regions of expected lap-splice performance per Eq. [1], while data within Quadrant II indicate excess conservatism. Data in Quadrant II primarily include lap-splice tests with No. 6 or smaller bars, for which Eq. [1], as aforementioned, produces conservatism due to the definition of γ. Quadrant IV indicates unconservative performance. Data located on the vertical line of $\frac{L_{d,prov}}{L_{d,calc}} = 1.15$ indicate lap-splice tests that were designed with $\Psi_g = 1.15$ in Eq. [1] and satisfied or exceeded the design criterion of $1.15f_y$. Similarly, overly conservative results on this line, i.e., $\frac{f_{s,max}}{f_y} \gg 1.15$, are associated with lap splices of smaller bars.

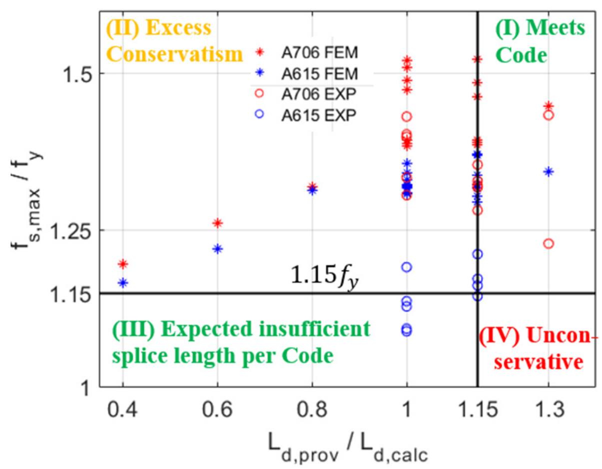

Figure 5: Summary of Grade 80 lap-splice performance; $f_{s,max}$ = maximum measured rebar stress in the test; $L_{d,prov}$ = lap-splice length provided in the test; $L_{d,calc}$ = maximum lap-splice length estimated from Eq. [1]; FEM = Finite Element Analysis; EXP = Experiment.

OUT-OF-PLANE WALL BEHAVIOR WITH GRADE 80 BARS

A set of eleven flexural tests of fully and partially grouted, concrete and clay brick masonry, walls has been completed at the University of Houston. The walls were subjected to four-point bending, using the test setup of Fig. 6. The tests were performed with the use of a frame system that supported a vertical MTS 55-kip (245-kN) capacity double acting actuator. A loading plate and a steel beam were used between the actuator to distribute the load on two rollers that simulated the two loading points. The walls were supported on the laboratory's strong floor with two steel beams and plates. Two roller supports were included between the walls and the floor beams. The actuator was laterally restrained to prevent any lateral movements during load application, as shown in Fig. 7a.

Fabrication of the walls was performed in the Structural Research Laboratory at the University of Houston with support by local professional mason groups. Upon fabrication, several companion material specimens were collected and tested for quality control. The tests were performed using a monotonic load application. During the first 10-kN of actuator loading, the actuator operated in load control and switched to displacement control right after and until the wall failure. As briefly described in Fig. 6, the walls were instrumented with a set of string potentiometers to measure the vertical deflection at distributed points. An additional set of light emitting diode (LED) markers were mounted on the wall to track three-dimensional movements during deflection and estimate the tensile and compressive cross-sectional deformations along the wall length. Strain gauges were mounted on different bar sides and locations near the wall mid-span.

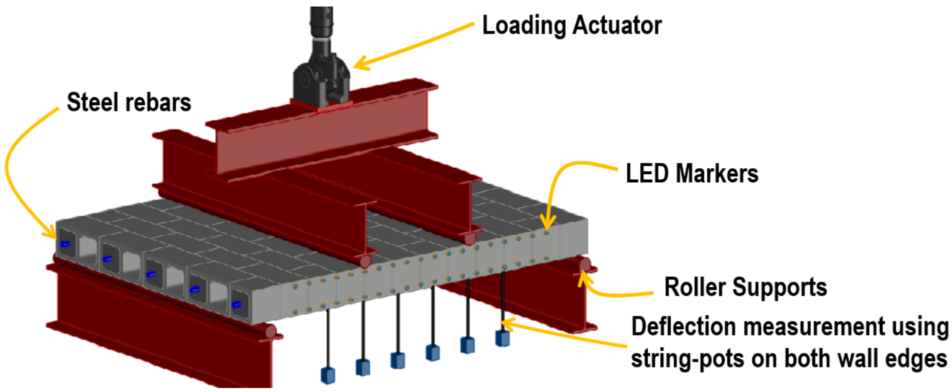

Figure 6: Out-of-plane wall test setup in the University of Houston.

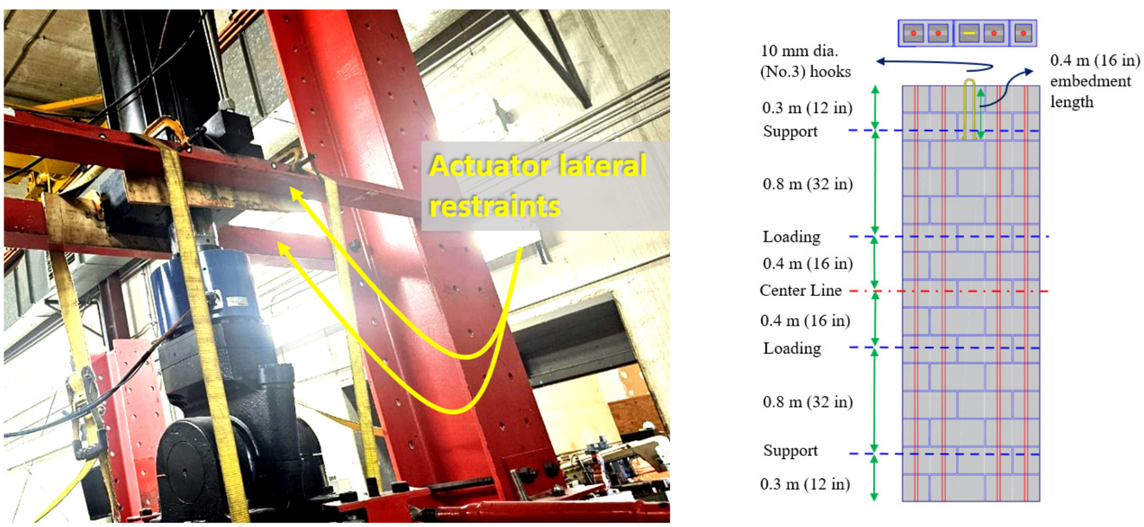

(a) Lateral restraints used for the actuator **(b) Example of wall design**

Figure 7: Actuator lateral restraints and example of wall design with location of support and loading points.

Each wall span from support to support was 2.4 m (96 inches) and the two loading points were placed at 0.8 m (32 inches), as shown in Fig. 7b. To accommodate the development length of the bars, outside of the loading region, most of the walls were extended beyond the 2.4 m of the support-to-support distance. In some cases, this extension length was 0.3 m (12 inches), less, or more, depending on the required development length of the bars. As shown in Fig. 7b, No. 3 bar hooks were included at one end of the wall to facilitate wall transportation, lifting, and placement in the laboratory setup.

The test matrix is shown in Table 2. The walls were designed to be in tension-control, transition, and compression-control as defined in TMS 402-22. The walls were fabricated with 8 in. x 8 in. x 16 in. (width x height x length) concrete masonry units (CMU) and 8 in. x 4 in. x 16 in. (width x height x length) clay bricks (CB), with partially and fully grouted configurations. One wall (Wall-1) used Grade 60 bars, while all other walls used Grade 80 bars. One of the walls, Wall-8, was tested under three-point bending (3PBT).

The walls were fabricated with No. 5 and No. 7 bars and the masonry strength, f'_m, varied from 18.6 MPa (2.7 ksi), for the CMU walls, to 27.6 MPa (4 ksi), for the CB walls. The walls were reinforced only with longitudinal bars; no transverse reinforcement was included. Wall-8 and Wall-11 had the longitudinal bars spliced (SP) at the mid-span, while all other walls used single continuous bars throughout the wall span.

Table 2: Test matrix of out-of-plane wall tests.

#	Wall Name	Masonry strength, f'_m, MPa (ksi)	Number of reinforcing bars	Grouting	Controlling Response per TMS 402-22	Bar Grade and Size
1	Wall-1-CMU-No5-4-Gr60-PG	18.6 (2.7)	4	Partially grouted	Tension	60, No. 5
2	Wall-2-CMU-No5-2-Gr80-PG	18.6 (2.7)	2	Partially grouted	Tension	80, No. 5
3	Wall-3-CMU-No5-3-Gr80-FG	18.6 (2.7)	3	Fully grouted	Tension	80, No. 5
4	Wall-4-CMU-No5-4-Gr80-FG	18.6 (2.7)	4	Fully grouted	Transition	80, No. 5
5	Wall-5-CMU-No7-2-Gr80-PG	18.6 (2.7)	2	Partially grouted	Transition	80, No. 7
6	Wall-6-CMU-No7-3-Gr80-PG	18.6 (2.7)	3	Partially grouted	Compression	80, No. 7
7	Wall-7-CMU-No7-3-Gr80-PG-FR	18.6 (2.7)	3	Partially grouted	NA	80, No. 7
8	Wall-8-CMU-No7-1-Gr80-3PBT-SP	18.6 (2.7)	1	Partially grouted	Tension	80, No. 7
9	Wall-9-CB-No5-4-Gr80-PG	27.6 (4.0)	4	Partially grouted	Tension	80, No. 5
10	Wall-10-CB-No7-3-Gr80-PG	27.6 (4.0)	3	Partially grouted	Tension	80, No. 7
11	Wall-11-CB-No7-4-Gr80-PG-SP	27.6 (4.0)	4	Partially grouted	Transition	80, No. 7

Table Notes: Wall-8 included a single lap-spliced bar and was tested under three-point bending, while all other walls were tested under four-point bending; FG = Fully Grouted; PG = Partially Grouted; No = Bar Size; Gr60 = Grade 60; Gr80 = Grade 80; Masonry strength f'_m was calculated using the unit strength method in TMS 602-22; FR = Wall-7 included steel fibers in the grout mix at a 1.0% volumetric ratio; NA = Not applicable, since Wall-8 used fiber-reinforced grout, which falls outside of TMS 402 provisions.

Test Results

Table 3 presents a summary of the wall responses along with the strength design estimates of flexural nominal load per TMS 402-22, where the maximum nominal bar stress was assumed as 80,000 psi. The table also includes flexural strength estimates per TMS 402-22 (P_{nf}) and comparisons with the experimental values (P_{exp}), where P denotes the applied actuator force. TMS 402-22 estimated wall flexural strengths below the experimental values in all walls, except Wall-11, which is expected because the experimental values incorporate the overstrength of the walls which can originate from several sources. In the tension-controlled walls, the overstrength is due to the strain-hardening behavior of the bars, which is not included in the code-based equations. The unconservative estimate for Wall-11 is attributed to the complex failure mode exhibited in this wall, as per Table 4, combined with the shear strength being close to the flexural strength (i.e., P_{nv} = 169 kN [38 kips]), creating some uncertainty in the wall dominating behavior. This uncertainty is, however, eliminated in design by means of the strength reduction factors.

The code-based estimates became more conservative for walls that exhibited compression-dominated failures. These failures initiated by crushing of the compression flanges, which propagated into a diagonal compression strut, creating an arching action and subsequent shear failure. Table 4 presents a general description of the response and failure mode for each of the tested walls. Overall, TMS 402-22 was able to predict most of the controlling responses, it provided satisfactory estimates of nominal load and can be reliably used for the flexural design of reinforced masonry with Grade 80 bars.

Table 3: Summary of out-of-plane wall test results and comparisons with TMS 402-22.

#	Wall Name	P_{nf}, kN (kips)	P_{exp}, kN (kips)	P_{exp}/P_n
1	Wall-1-CMU-No5-4-Gr60-PG	63.6 (14.3)	89.4 (20.1)	1.40
2	Wall-2-CMU-No5-2-Gr80-PG	43.1 (9.7)	50.7 (11.4)	1.17
3	Wall-3-CMU-No5-3-Gr80-FG	62.7 (14.1)	67.6 (15.2)	1.08
4	Wall-4-CMU-No5-4-Gr80-FG	82.3 (18.5)	87.2 (19.6)	1.06
5	Wall-5-CMU-No7-2-Gr80-PG	84.1 (18.9)	91.6 (20.6)	1.09
6	Wall-6-CMU-No7-3-Gr80-PG	115.7 (26)	163.2 (36.7)	1.41
7	Wall-7-CMU-No7-3-Gr80-PG-FR	-	134.8 (30.3)	-
8	Wall-8-CMU-No7-1-Gr80-3PBT-SP	27.6 (6.2)	38.7 (8.7)	1.41
9	Wall-9-CB-No5-4-Gr80-PG	88.1 (19.8)	107.6 (24.2)	1.22
10	Wall-10-CB-No7-3-Gr80-PG	125 (28.1)	156.1 (35.1)	1.25
11	Wall-11-CB-No7-4-Gr80-PG-SP	157.9 (35.5)	140.1 (31.5)	0.89

Table Notes: No P_{nf} is provided for Wall-7, because TMS 402-22 does not account for the contribution of steel fibers in the flexural strength calculations.

Fig. 8 presents examples of force-deflection curves from two tested walls, featuring tension- and compression-controlled responses, along with the corresponding TMS 402-22 nominal load estimates.

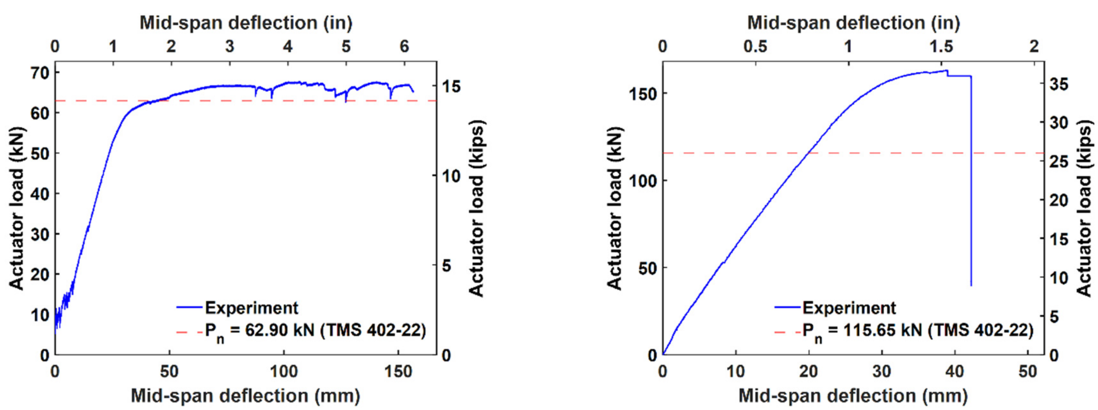

(a) Wall-3-CMU-No5-3-Gr80-FG **(b) Wall-6-CMU-No7-3-Gr80-PG**

Figure 8: Examples of load versus deflection responses for Wall-3 and Wall-6.

Fig. 9 presents example responses near failure for two of the test specimens. Wall-3 below exhibited large flexural deflections which were eventually localized within a mortar joint between the loading points. The mortar joint experienced a large crack opening and failure occurred due to crushing of the CMU flange in the compression zone. Wall-6 experienced a compression-controlled failure. The failure was initiated by crushing of the top flange near the point of load application. The crushing was quickly followed by arching action that led to a compression shear failure.

Table 4: Classification of wall responses.

#	Wall Name	Controlling Response per TMS 402-22	Description of experimental failure
1	Wall-1-CMU-No5-4-Gr60-PG	Tension	Significant flexural crack opening, followed by large tensile strains in rebars and eventual crushing of the CMU flange under large flexural deformations. Δ_u = 11.9 cm.
2	Wall-2-CMU-No5-2-Gr80-PG	Tension	Similar observations to Wall-1. Δ_u = 12.9 cm.
3	Wall-3-CMU-No5-3-Gr80-FG	Tension	Similar observations to Wall-1. Δ_u = 15.5 cm.
4	Wall-4-CMU-No5-4-Gr80-FG	Transition	Moderate flexural crack opening, followed by crushing of CMU flange. Failure was combined with a splitting horizontal crack within the compression zone near the mid-span. Δ_u = 8.3 cm.
5	Wall-5-CMU-No7-2-Gr80-PG	Transition	Similar observations to Wall-4. Δ_u = 7.9 cm.
6	Wall-6-CMU-No7-3-Gr80-PG	Compression	Crushing of the CMU flange, which was followed by a compression shear failure with diagonal cracks propagating to the supports at small flexural deformations. Δ_u = 4.2 cm.
7	Wall-7-CMU-No7-3-Gr80-PG-FR	-	Crushing of the CMU flange followed by a longitudinal splitting crack along a mortar joint next to the ungrouted cell. A minor diagonal crack developed partially toward the support during failure. Small flexural crack openings and small flexural deformations. Δ_u = 4.2 cm.
8	Wall-8-CMU-No7-1-Gr80-3PBT-SP	Tension	A distinct flexural crack developed below the loading point followed quickly by crushing of the CMU flange and a longitudinal splitting crack along a mortar joint next to the ungrouted cell. A bursting failure followed, splitting the wall in the longitudinal direction. Δ_u = 3.1 cm.
9	Wall-9-CB-No5-4-Gr80-PG	Tension	Similar observations to Wall-1. Δ_u = 9.3 cm.
10	Wall-10-CB-No7-3-Gr80-PG	Tension	Similar observations to Wall-6. The failure was combined with delamination between the CB compression flange and the grouted cells. Δ_u = 4.8 cm.
11	Wall-11-CB-No7-4-Gr80-PG-SP	Transition	A horizontal splitting crack initiated within the compression zone and developed into a diagonal crack toward the support. This occurred simultaneously with a longitudinal splitting crack. Additional splitting cracks developed within the compression zone near the support, which was followed by delamination of the CB flange from the grouted cells and growth of the diagonal crack. Failure occurred due to the combined delamination effect and a diagonal tension failure. Δ_u = 3.1 cm.

Table Notes: Δ_u is the ultimate deflection at mid-span as recorded just before the wall failure.

(a) Wall-3-CMU-No5-3-Gr80-FG

(b) Wall-6-CMU-No7-3-Gr80-PG

Figure 9: Photographs taken near wall failures.

CONCLUSIONS

The University of Houston research program on HSRBs has so far produced a significant set of lap-splice and flexure test data for the use of Grade 80 A706 and A615 bars in concrete and clay brick masonry. The program will continue with axial load and shear tests to provide a comprehensive characterization that will pave the way for code adoption of HSRBs by TMS 402/602 and elsewhere.

Based on the existing experimental and numerical analysis data, the project team proposed a grade factor of $\Psi_g = 1.15$ for use in the existing lap-splice equation of TMS 402 with an associated reduced design criterion of $1.15 f_y$ for spliced Grade 80 bars in low-seismic regions. Based on a comprehensive rebar test series reported in [10] and elsewhere, this criterion is sufficient to reliably surpass the upper yield point of Grade 80 bars and satisfy the TMS 402-22 strength design assumptions. It is also noted that the use of $\Psi_g = 1.15$ is the same as the grade factor adopted for Grade 80 bars by the reinforced concrete industry [1].

The lap-splice tests corroborated the need to revisit the definition of the bar size factor, γ, in Eq. [1]. This factor produces overly conservative lengths for smaller bar sizes and liberal lengths for larger bars. Future code revisions are needed to improve the accuracy in the calculation of γ, regardless of the bar grade.

Finally, the out-of-plane wall tests showed that the TMS 402/602-22 provisions can be extended to the flexural design of masonry with Grade 80 bars. Comparisons between TMS 402/602 estimates and experimental data showed that Grade 80 bars meet code expectations of flexural nominal strength and classification requirements in terms of tension- and compression-control with acceptable accuracy.

ACKNOWLEDGEMENTS

The authors acknowledge the (1) National Concrete Masonry Association (NCMA) and Western States Clay Products Association (WSCPA); (2) Texas Masonry Council (TMC) and its Executive Director Tony Topping; (3) BarSplice Products Inc., Concrete Reinforcing Steel Institute, Interstate Brick, Best Block Construction Materials, Nucor Harris Rebar, and D'Ambra Construction; and (4) Veazey Enterprises. The authors also acknowledge John Hochwalt for serving as the industry advisor in this project.

REFERENCES

[1] ACI 318 (2019). “Building code requirements for structural concrete (ACI 318-19) and commentary (ACI 318R-19).” *American Concrete Institute*, Farmington Hills, MI.

[2] ASTM A706/A706M-16 (2016). “Standard specification for deformed and plain low-alloy steel bars for concrete reinforcement.” *American Society for Testing and Materials*. West Conshohocken, Pennsylvania.

[3] ASTM A615/A615M-18 (2018). “Standard specification for deformed and plain carbon-steel bars for concrete reinforcement.” *American Society for Testing and Materials*. West Conshohocken, Pennsylvania.

[4] Khalid, O. and Kalliontzis, D. (2023). “High-strength reinforcing bars (HSRBs) and TMS 402: A first study on Grade 80 bars.” *TMS Journal*, 41(1), 39-60.

[5] ASTM A370-21 (2021). “Standard test methods and definitions for mechanical testing of steel products,” *American Society for Testing and Materials*, West Conshohocken, Pennsylvania.

[6] TMS 402/602 (2022). “Building code requirements and specification for masonry structures.” *The Masonry Society*, Logmont, Colorado.

[7] Khalid, O., Khan, W. and Kalliontzis, D. (2024). “Evaluating lap-splice length requirements for Grade 80 deformed bars in structural masonry.” *ASCE Journal of Structural Engineering*, 151(3), https://doi.org/10.1061/JSENDH.STENG-13571.

[8] Thompson, J. J. (1997). "Behavior and design of tension lap splices in reinforced concrete masonry." *MSc Thesis*, Department of Civil and Environmental Engineering, Washington State University.
[9] Carvalho, E. P., Miranda, M. P., Fernandes, D. S. G. and Alves, G. V. (2018). "Comparison of Test Methodologies to Evaluate Steel-Concrete Bond Strength of Thin Reinforcing Bars." *Construction and Building Materials*, 183, 243-252.
[10] Schultz, A. E. (2005). "An evaluation of reinforcing bar splice requirements for strength design of masonry structures." *A report to the Council for Masonry Research (CMR)*, AES Engineering, Deephaven, MN.
[11] Overby, D., Kowalsky, M. and Seracino, R. (2017). "Stress-Strain Response of A706 Grade 80 Reinforcing Steel." *Construction and Building Materials*, 145, 292-302.